Visually Lossless JPEG 2000 Decoder

Leandro Jiménez-Rodríguez†, Francesc Aulí-Llinàs†,
Michael W. Marcellin‡, and Joan Serra-Sagristà†

† Department of Information and Communications Engineering
Universitat Autònoma de Barcelona, Barcelona, Spain
‡ Department of Electrical and Computer Engineering
University of Arizona, Tucson, AZ, USA

Abstract

Visually lossless coding is a method through which an image is coded with numerical losses that are not noticeable by visual inspection. Contrary to numerically lossless coding, visually lossless coding can achieve high compression ratios. In general, visually lossless coding is approached from the point of view of the encoder, i.e., as a procedure devised to generate a compressed codestream from an original image. If an image has already been encoded to a very high fidelity (higher than visually lossless – perhaps even numerically lossless), it is not straightforward to create a "just" visually lossless version without fully re-encoding the image. However, for large repositories, re-encoding may not be a suitable option. A visually lossless *de*coder might be useful to decode, or to parse and transmit, only the data needed for visually lossless reconstruction. This work introduces a decoder for JPEG 2000 codestreams that identifies and decodes the minimum amount of information needed to produce a visually lossless image. The main insights behind the proposed method are to estimate the variance of the codeblocks before the decoding procedure, and to determine the visibility thresholds employing a well-known model from the literature. The main advantages are faster decoding and the possibility to transmit visually lossless images employing minimal bitrates.

I. Introduction

The last decades have experienced astounding growth in the use of images due to powerful capturing sensors such as those found in digital cameras, medicine instruments, or remote sensing devices. This has resulted in large repositories of images that have to be stored and transmitted, bringing new techniques and standards to compress such data sets efficiently. In general, images are encoded using a lossy or lossless coding scheme that permits the recovery of the original image with or without information loss, respectively. Lossless, or numerically lossless, methods commonly achieve moderate compression ratios, whereas lossy methods achieve higher compression ratios at the expense of image fidelity. In the last years, a new image compression modality employing the best of these two types of compression regimes has appeared. This modality is commonly called visually lossless coding due to its ability to compress an image making use of lossy coding techniques in such a way that the information loss is not noticeable by the human visual system (HVS). The main advantage of visually lossless coding methods is that they achieve compression ratios higher than those achieved by numerically lossless techniques, but look to a human observer as if they were compressed losslessly, i.e., without any loss in quality.

Typically, the first step in the implementation of a visually lossless coding scheme is to model the HVS. One approach to do so is to employ the contrast sensitivity function (CSF), which models the sensitivity of the human eye to contrast variations as a function of spatial frequency. The CSF has been measured with psychophysical experiments in order to find the just-noticeable points (i.e., the visibility thresholds) of a stimulus in a predefined contrast unit. The CSF varies depending on the age and the visual acuity of the subject, as well as on the viewing conditions and the stimuli used in the experiments [1], [2]. Typically, the stimuli employed to measure the sensitivity are generated with transforms that simulate the neurons of the primary visual cortex reception fields (V1) of the HVS. These reception fields are well described by the Gabor filter [3], which is ideal for space-frequency localization, albeit at high computational complexity. An alternative to the Gabor filter is to use the cortex transform proposed by Watson [4], which is invertible, easy to implement, and models V1 accurately and with adjustable parameters. Though being an appropriate tool to model the HVS, the cortex transform is not suitable to image compression because it increases the number of encoded coefficients [5]. Consequently, other transforms such as the discrete cosine transform (DCT) or the discrete wavelet transform (DWT) are more commonly employed in perceptual image compression.

The DWT is a decorrelation technique that has been utilized in vision models [6], [7] due to its well-posed properties for the HVS such as linearity, invertibility, and logarithmically spaced spatial frequencies divided in four orientations. Also, the DWT is one of the most popular transforms employed to perform image compression due to its decorrelation properties, which allow the attainment of high compression ratios. The JPEG 2000 standard [8], for example, utilizes the DWT as the first stage of the coding system. The use of the DWT in JPEG 2000 has permitted the deployment of techniques compatible with the standard that are aimed at the perceptual coding of images [9], [10]. These techniques yield improved visual quality, but are not able to ensure visually lossless performance. In one of the early steps in this direction, Watson et al. measured the visibility thresholds (VTs) for individual wavelet subbands using randomly generated *uniform* noise as a substitute for quantization error [11]. The resulting VTs can then be employed in wavelet-based coding schemes to code the coefficients in the wavelet subbands until the threshold for that subband is reached.

Unfortunately, the use of uniform noise to obtain the VTs of [11] results in non-visually lossless results when these VTs are employed in JPEG 2000 [12]. This is because JPEG 2000 employs a dead-zone uniform scalar quantizer which results in non-uniform quantization noise. Other approaches to obtain VTs (such as [13], [14]) achieve more accurate thresholds, though they still assume uniform noise and/or uniform quantization. A more suitable model of quantization noise for JPEG 2000 was proposed in [15]. Through that model, compressed images are produced that are indistinguishable from the original ones. Furthermore, the coding scheme proposed in [15] achieves superior compression ratios compared to previous visually lossless work done in the framework of JPEG 2000 [16].

The main trend in perceptual image coding has pursued increased accuracy of the HVS model to achieve higher compression ratios without affecting the perceptual quality of images. The main advantages of visually lossless methods are that the images look identical to the original ones, that the coding process can be faster because only the visually relevant information is coded, and that images can be transmitted employing less channel bandwidth. Nonetheless, there exist large repositories of images that have already been encoded using numerically lossless or (very high fidelity) lossy methods. Most perceptual coding methods in the literature are devised from the point of view of the encoder. Unless the encoder has specifically envisioned it [17], there is generally no mechanisms to decode, or to parse and transmit, a visually lossless image from an already compressed codestream without performing a full decoding and re-encoding. To re-encode all images of large repositories may not be viable due to computational costs, so in some cases the benefits of visually lossless coding methods can not be exploited.

The purpose of this work is to introduce a visually lossless decoder that is able to identify and decode, or parse and transmit, only the information necessary to reconstruct a visually lossless image from a codestream encoded using a conventional JPEG 2000 encoder. The main insights behind the proposed method are to employ variance estimates that only require the decoding of codestream headers, and the use of the perceptual model of [15] to determine VTs.

The paper is organized as follows. Section II overviews the model employed to determine the VTs, and describes the proposed visually lossless JPEG 2000 decoder. Section III appraises the performance of the proposed method through experimental results that assess decoding rate and computational time reduction. The last section summarizes this work and draws lines of future research.

II. Visually lossless decoder for JPEG 2000

A. Determination of visibility thresholds

An important aspect behind the visually lossless method proposed in [15] is the model of quantization distortion employed, which captures with high accuracy the quantization error produced by a dead-zone uniform quantizer. Previous works assumed uniform error over the interval $(-\Delta/2, \Delta/2)$. Instead, [15] models the quantization error of high frequency wavelet subbands (i.e., subbands containing the High-vertical Low-horizontal frequencies (HL), or LH, or HH) by the probability density function (pdf)

$$f(d) = \begin{cases} g(d) + \dfrac{1 - \int_{-\Delta}^{\Delta} g(y)dy}{\Delta} & \text{if } 0 \leq |d| \leq \frac{\Delta}{2} \\ g(d) & \text{if } \frac{\Delta}{2} < |d| \leq \Delta \\ 0 & \text{otherwise} \end{cases}, \tag{1}$$

where $g(\cdot)$ denotes the pdf of coefficients d in a wavelet subband. In [15], $g(\cdot)$ is approximated as a Laplacian distribution with parameters $\mu = 0$ and variance σ^2. Δ is the step size of the quantizer. The first term in the two first lines of (1) indicate that the quantization error produced for coefficients within the deadzone interval (i.e., $(-\Delta, \Delta)$) is equal to the coefficients themselves, since they are reconstructed as zero. The second term in the first line of (1) arises from assuming that wavelet coefficients with $|d| > \Delta$ produce uniformly distributed errors. The resulting density function is depicted in Fig. 1. The low-frequency subband (i.e., LL) is modeled similarly.

This model of quantization distortion is employed to determine VTs for wavelet subbands. To do so, a stimulus image is generated by applying the inverse DWT to wavelet data that contain simulated quantization distortions. The (simulated) quantization distortion is generated in one wavelet subband employing the model of (1) for an assumed coefficient variance and quantization step size Δ. The inverse DWT then produces an

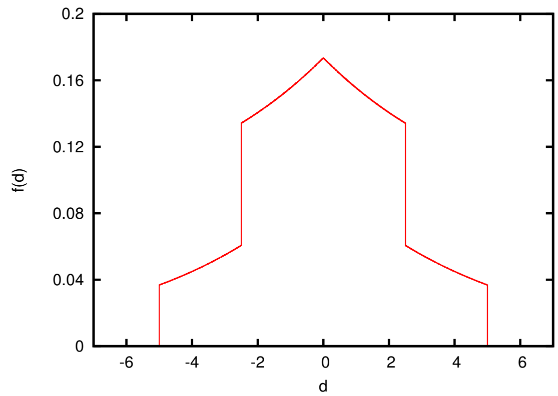

Fig. 1: Model of quantization distortion introduced in [15]. The pdf of wavelet coefficients $f(d)$ is modeled as a Laplacian distribution with parameters $\mu = 0$ and $\sigma^2 = 50$. The step size of the quantizer is $\Delta = 5$.

image with a distortion corresponding to quantization error for that subband, variance, and step size. To determine the VT for the subband and variance, a two-alternative forced choice method is used. In this method, the stimulus image and a mid-gray level image are displayed together and a human subject must decide which is the stimulus image. The experiment is iterated varying the step size Δ to find the largest Δ in which the stimulus image can not be distinguished from the mid-gray level image. Δ is determined after 32 iterations of the QUEST staircase procedure described in the Psychophysics Toolbox [18].

In [15], VTs were measured in this fashion for a small set of different values of variance in each subband. A piecewise linear function was then employed to model VTs for different values of variance. In this work, we have employed the same procedure to determine the VTs for a set of variance values in each wavelet subband. However, instead of employing a piecewise linear model for other values of variance, we employ the following logarithmic function

$$\mathrm{VT}(\sigma^2) = (\mathrm{VT}_{max} - \mathrm{VT}_{min}) \cdot \left(1 - \frac{B^{1-\frac{\sigma^2-\sigma^2_{min}}{\sigma^2_{max}}} - 1}{B-1}\right) + \mathrm{VT}_{min} \ , \tag{2}$$

where VT_{max} is the VT determined experimentally for the maximum variance σ^2_{max} employed for the subband, and VT_{min} is the VT determined experimentally for the minimum variance σ^2_{min}. B determines the shape of the logarithmic function, and is selected to fit the VTs of the subband. Similar to [15], we have determined 5 VTs for each subband corresponding to $\sigma^2 = 5, 50, 100, 175,$ and 300. The parameter B has then been selected to fit the experimentally achieved thresholds.

Fig. 2 depicts the VTs determined for two different wavelet subbands together with the resulting models obtained via (2). Results for other subbands are similar. Table I reports the model parameters obtained for all subbands corresponding to 5 levels of irreversible 9/7 wavelet transform. Subbands HL and LH are reported together since the same VTs

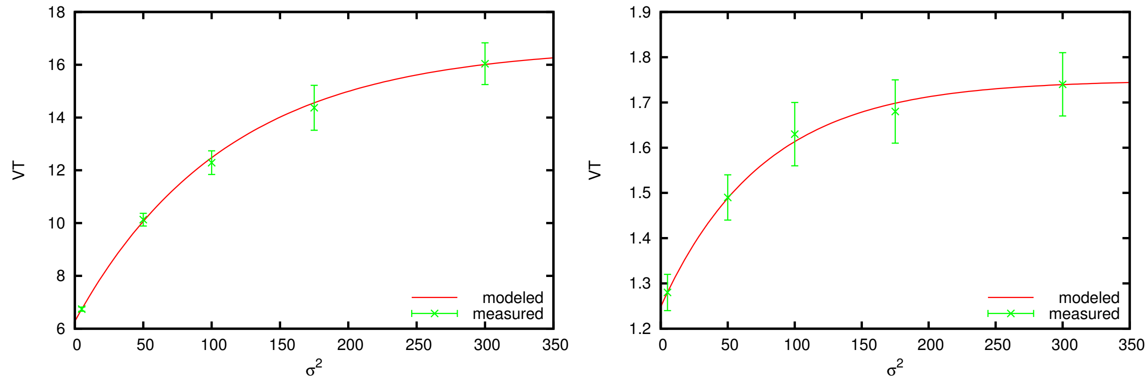

(a) HH_1 (b) HL/LH_2

Fig. 2: Modeling of the VTs determined for wavelet subbands generated by the irreversible 9/7 CDF wavelet transform defined in JPEG 2000. The green points are the VTs determined for five different levels of variance, with the green bars showing ± 1 standard deviation. The red plot depicts the model of Equation (2).

TABLE I: Parameters employed in Equation (2) for each wavelet subband and decomposition level.

	HH			HL/HL		
Level	VT_{min}	VT_{max}	B	VT_{min}	VT_{max}	B
1	6.74	16.04	15	4.00	9.81	25
2	1.83	2.70	30	1.28	1.74	50
3	1.22	1.63	60	0.96	1.24	100
4	1.07	1.41	120	0.93	1.12	200
5	1.06	1.38	240	0.74	0.97	400

are achieved for both. As in [15], the LL subband is assigned a single VT regardless of the variance. The value employed here is 0.81.

B. Decoding procedure

The main stages of a typical JPEG 2000 encoder implementation are: data transformation, data coding, rate-distortion optimization, and codestream re-organization. The first stage transforms the image samples through a wavelet transform and quantizes wavelet coefficients employing a deadzone uniform scalar quantizer with step size Δ. The quantization indices are then grouped in small sets, called codeblocks, that are coded in the second stage by means of a fractional bitplane coding engine that carries out three coding passes per bitplane. One bitplane is defined as the collection of bits from all indices corresponding to the same position of their binary representation. JPEG 2000 and most modern image coding systems code wavelet data in a bitplane-by-bitplane fashion due to its inherent embedding and excellent coding performance. In JPEG 2000 each codeblock is coded independently, producing a quality progressive bitstream that can be truncated at certain points. Rate-distortion optimization is commonly used to attain a target rate for the final codestream, or to construct quality layers. The main idea behind the optimization process of JPEG 2000 is to selectively include the bitstream segments of codeblocks in the final codestream employing a rate-distortion criterion. The final stage codes auxiliary information and organizes the final codestream using a progression order.

Commonly, the decoding procedure decodes the bitstream corresponding to a codeblock from the most significant bitplane of the codeblock to the least significant bitplane, or until the last coding pass included in the codestream for that codeblock is reached. Rather than decoding all available coding passes from the codeblock, the proposed method stops the decoding procedure upon reaching that bitplane which lies just below the VT determined for that subband. Specifically, let the bitplanes be numbered starting with 0 for the least significant. Then, decoding (starting with the most significant bitplane) is terminated after decoding the earliest bitplane P such that $\Delta 2^P \leq \mathrm{VT}(\sigma^2)$, with Δ denoting the quantization step size of the subband. In practice, the decoder computes P as

$$P = \left\lfloor log_2 \frac{\mathrm{VT}(\sigma^2)}{\Delta} \right\rfloor \; . \tag{3}$$

Evidently, if the codestream does not contain enough coding passes to reach bitplane P, the decoder stops the procedure at the last available coding pass and then visually lossless quality can not be guaranteed.

The main difficulty to apply the above procedure in practice is that the variances of the codeblocks are not available from the compressed codestream. Variances are not needed to decode the image and so to keep them in the codestream would unnecessarily increase its length. Variances could be estimated via decoding of the whole codestream, but this largely defeats the purpose of the present work. So an alternative estimate of these variances is required. It is important that the employed approach does not require the inclusion of additional information in the codestream since our goal is to obtain a decoder able to handle already encoded images. One piece of information relevant to the variance of a codeblock that can be obtained without decoding any bitplane data is the bitplane number of the most significant bitplane M, which is coded in the headers of the codestream. As seen below, M can be used to provide a reasonable estimate for the variance of a codeblock.

Fig. 3 reports the average variance for codeblocks found in the wavelet subbands for a large collection of wavelet-transformed images. Each point in the plot corresponds to the average variance of codeblocks in one wavelet subband that have the same value of M. The results indicate that the variance of codeblocks is strongly related to the wavelet subband and to the bitplane number of the most significant bitplane of the codeblock. Note, for instance, that the average variance of codeblocks with $M < 4$ is almost zero for all subbands, and then the variance increases exponentially as M grows. The proposed decoder employs the average variances reported in Fig. 3 as estimates.

In summary, the proposed decoder works as follows. First, the bitplane number of the most significant bitplane M for a given codeblock is extracted from the codestream headers. Second, the variance of the codeblock is estimated through a lookup table containing the average variances reported in Fig. 3. The wavelet subband of the codeblock and M are used as the indices of this lookup table. Third, the VT for the codeblock is

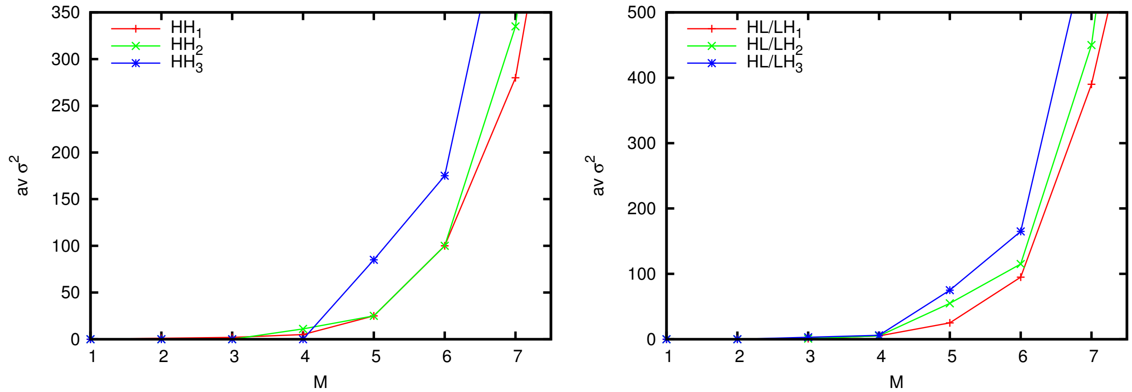

(a) HH subbands

(b) HL/LH subbands

Fig. 3: Evaluation of the variance of wavelet coefficients in codeblocks depending on their most significant bitplane M, for wavelet subbands produced by 5 levels of decomposition with the irreversible 9/7 CDF wavelet transform. Results are reported as the average variance of all codeblocks with same M, for the 24 images reported in Section III. Decomposition levels 4 and 5 are not depicted since the average variances obtained are higher than 500.

computed using the variance estimate and Equation (2). Fourth, the last bitplane P that the coding engine has to decode for that codeblock is computed via Equation (3). Fifth, the codeblock is decoded from bitplane M to bitplane P. This process is repeated for each codeblock to be decoded.

III. Experimental results

The experimental results carried out to assess the performance of the visually lossless JPEG 2000 decoder employ 24 images from different image corpora. All images are 8 bit, grayscale, with different sizes. Table II reports in the first two columns the images employed in this experiment as well as their sizes. We have not employed large images because the validation procedure described below requires the visualization of 3 versions of the same image simultaneously on the screen. The visually lossless decoder has been implemented in our JPEG 2000 codec BOI [19]. Coding parameters are: 5 levels of wavelet transform, codeblock size of 64×64, and a single quality layer codestream. The results for numerically lossless compression are achieved employing the reversible 5/3 CDF wavelet transform, whereas the remaining results are achieved employing the irreversible 9/7 CDF wavelet transform. The base quantization step size corresponding to bitplane 0 when the 9/7 filter-bank is used are chosen according to the L_2-norm of the synthesis basis vectors of the subband.

The first test validates that the images decoded by the proposed method are visually lossless. A three-alternative forced-choice (3AFC) procedure is used. In this procedure two original images and one decompressed image are displayed side by side on the screen with the position of the decoded image selected randomly. A subject is asked to choose the image which looks different. For each image, the test is repeated 5 times and the

image	size	NL	coder	decoder	[15]
barbara	512 × 512	4.66	2.00	-0.02	1.73
boat	512 × 512	4.01	1.90	-0.09	-
frog	621 × 498	6.25	3.74	+0.08	-
goldhill	512 × 512	4.84	2.51	-0.17	-
lena	512 × 512	4.32	1.87	-0.07	1.43
baboon	512 × 512	6.11	3.49	-0.07	2.70
mountain	640 × 480	6.70	3.85	-0.03	-
peppers	512 × 512	4.62	2.20	-0.23	1.61
zelda	512 × 512	3.99	1.56	-0.06	-
Woman	600 × 800	3.10	1.12	-0.04	-
Portrait	600 × 750	4.69	2.07	-0.15	-
Flowers	600 × 800	3.35	1.34	-0.13	-
Cafeteria	600 × 750	6.10	3.27	-0.02	-
Fishing goods	600 × 800	4.72	2.31	-0.18	-
Fruit Basket	600 × 750	4.48	1.98	-0.22	-
Japanese goods	600 × 800	5.07	2.64	-0.13	-
Tableware	600 × 750	4.50	1.73	-0.09	-
Field fire	600 × 800	4.53	2.22	-0.06	-
Bicycle	600 × 750	5.07	2.34	-0.10	-
Pier	600 × 800	4.79	2.37	-0.09	-
Orchid	600 × 750	3.53	1.08	-0.11	-
Threads	600 × 800	4.13	1.86	-0.08	-
Musicians	600 × 750	5.52	2.61	-0.11	-
Candle	600 × 750	6.15	3.23	-0.17	-
average	-	4.97	2.65	-0.10	-

TABLE II: Evaluation of the decoding rate achieved by the proposed decoder compared to a visually lossless encoder that uses same VTs. Results from [15] and results for numerically lossless (NL) encoding are also reported. All results are in bps.

subject has an unlimited time to examine the images. No viewing distance is enforced. A success ratio of $1/3$ would indicate that the images are visually lossless.

The 3AFC test is performed with a HP ZR2440w monitor that has an In-Plane Switching (IPS) panel, resolution of 1920×1200, static contrast ratio of 1:1000, brightness of 350 cd/m^2, and a dot pitch of 0.27mm. A total of 10 subjects participated in the validation test, making a total of 1200 validations. Images are first compressed with JPEG 2000 to a very high fidelity using the irreversible wavelet transform. Then, the decoder decompresses the visually relevant information from the codestream, discarding the remaining data. The mean frequency at which observers selected the correct image in this test was 0.343 with a standard deviation of 0.034. The achieved mean frequency is within one standard deviation of 1/3 and no outliers were detected, which suggest that the decoder produces visually lossless images.

Next, in the second test, the rate achieved by the proposed decoder is compared against the rate achieved by an encoder that uses the same method as that described for the decoder but using the real variances of the codeblocks. This test compares the accuracy of the variance estimates. The fourth column of Table II reports the rate achieved by the encoder, whereas the fifth column reports the difference between the decoder and encoder rates. Positive values in the fifth column indicate that the decoding rate is larger than the encoding rate. The achieved results suggest that the decoder is able to estimate variances with sufficient precision, resulting in a decoding rate only 0.10 bps less than that achieved by the encoder. The third and sixth columns of this table provide the results

image	NL	proposed	speed up
barbara	0.216	0.144	1.50
boat	0.212	0.139	1.53
frog	0.250	0.214	1.17
goldhill	0.216	0.161	1.34
lena	0.212	0.138	1.54
baboon	0.227	0.195	1.16
mountain	0.253	0.210	1.20
peppers	0.218	0.148	1.47
zelda	0.202	0.122	1.66
Woman	0.251	0.155	1.62
Portrait	0.278	0.191	1.46
Flowers	0.255	0.163	1.56
Cafeteria	0.312	0.237	1.32
Fishing goods	0.295	0.207	1.43
Fruit Basket	0.274	0.191	1.43
Japanese goods	0.296	0.217	1.36
Tableware	0.280	0.181	1.55
Field fire	0.287	0.207	1.38
Bicycle	0.295	0.209	1.41
Pier	0.291	0.212	1.37
Orchid	0.257	0.139	1.85
Threads	0.277	0.196	1.41
Musicians	0.301	0.216	1.39
Candle	0.314	0.174	1.81
average	0.261	0.182	1.46

TABLE III: Evaluation of the computational time employed by a numerically lossless (NL) decoder and the proposed visually lossless decoder. Results are reported in seconds.

achieved by a numerically lossless JPEG 2000, and those achieved in [15] for some of the images.

Compared to the numerically lossless method, the proposed decoder achieves significantly lower decoding rate. The codec introduced in [15] achieves higher compression ratios than those achieved by the proposed method. This is caused because [15] employs coding passes, instead of bitplanes, to decide when to stop the coding process, utilizes the real (sample) variance and distortion produced in each codeblock, and incorporates masking techniques to enhance the efficiency of the perceptual model. We note that, as originally formulated, these techniques can only be used in the encoder.

The third test is aimed to evaluate the computational time savings achieved when the proposed method is employed. Computational time results are obtained with an Intel Core2 Duo CPU at 3 GHz. BOI is implemented in Java and is executed on a JVM version 1.6. Table III reports the computational time spent by the bitplane coding procedure, which is also called tier-1 in JPEG 2000, when decoding the image numerically losslessly, and visually losslessly. On average, the proposed decoder is approximately 46% faster than numerically lossless decoding. These results suggest that the proposed JPEG 2000 visually lossless decoder is able to accelerate the decoding process without penalizing the visual quality of the decoded image.

IV. Conclusions

Visually lossless coding prevents quality losses while achieving high compression ratios. In general, visually lossless coding methods assume that the original image is available. If the image is already coded, however, most methods are not able to identify the visually relevant information within the codestream without fully re-encoding the image. In this work we propose a method for the decoding of JPEG 2000 codestreams to produce visually lossless images. The main advantage of the proposed method is that it does not require re-encoding and so it can be employed to accelerate the decoding procedure or to transmit the image employing less bitrate than conventional methods. Future research is focused on the improvement of the perceptual model for the decoder by incorporating masking techniques as well as the inclusion of the proposed method in a JPIP-compliant server.

ACKNOWLEDGMENT

This work has been partially supported by the Universitat Autònoma de Barcelona, by the Spanish Government (MINECO), by the European Union, by FEDER, and by the Catalan Government, under Grants UAB-472-01-2/09, RYC-2010-05671, FP7-PEOPLE-2009-IIF-250420, TIN2009-14426-C02-01, TIN2012-38102-C03-03, and 2009-SGR-1224.

REFERENCES

[1] N. Graham, *Visual Pattern Analyzers*. New York: Oxford University Press, 1989.
[2] S. Daly, "Application of a noise-adaptive contrast sensitivity function to image data compression," *Optical Engineering*, vol. 29, no. 8, pp. 977–987, 1990.
[3] C. Taylor, Z. Pizlo, J. Allebach, and C. Bouman, "Image quality assessment with a gabor pyramid model of the human visual system," in *Electronic Imaging'97*. International Society for Optics and Photonics, 1997, pp. 58–69.
[4] A. Watson, "The cortex transform: rapid computation of simulated neural images," *Computer vision, Graphics, and Image Processing*, vol. 39, no. 3, pp. 311–327, 1987.
[5] D. Wu, D. Tan, M. Baird, J. DeCampo, C. White, and H. Wu, "Perceptually lossless medical image coding," *IEEE Transactions on Image Processing*, vol. 25, no. 3, pp. 335–344, 2006.
[6] M. Bolin and G. Meyer, "A perceptually based adaptive sampling algorithm," in *SIGGRAPH 99 Conference Proceedings*. ACM, 1998, pp. 299–309.
[7] M. Masry, S. Hemami, and Y. Sermadevi, "A scalable wavelet-based video distortion metric and applications," *IEEE Transactions on Circuits and Systems for Video Technology*, vol. 16, no. 2, pp. 260–273, 2006.
[8] D. S. Taubman and M. W. Marcellin, *JPEG2000 Image compression fundamentals, standards and practice*. Norwell, Massachusetts 02061 USA: Kluwer Academic Publishers, 2002.
[9] M. Nadenau and J. Reichel, "Opponent color, human vision and wavelets for image compression," in *Proceedings of the Seventh Color Imaging Conference*, 1999, pp. 237–242.
[10] W. Zeng, S. Daly, and S. Lei, "An overview of the visual optimization tools in JPEG2000," *Signal Processing: Image Communication*, vol. 17, no. 1, pp. 85–104, 2002.
[11] A. Watson, G. Yang, J. Solomon, and J. Villasenor, "Visibility of wavelet quantization noise," *IEEE Transactions on Image Processing*, vol. 6, no. 8, pp. 1164–1175, 1997.
[12] Z. Liu, L. Karam, and A. Watson, "JPEG2000 encoding with perceptual distortion control," *IEEE Transactions on Image Processing*, vol. 15, no. 7, pp. 1763–1778, 2006.
[13] M. Ramos and S. Hemami, "Suprathreshold wavelet coefficient quantization in complex stimuli: psychophysical evaluation and analysis," *Journal of the Optical Society of America A*, vol. 18, no. 10, pp. 2385–2397, 2001.
[14] D. Chandler and S. Hemami, "Dynamic contrast-based quantization for lossy wavelet image compression," *IEEE Transactions on Image Processing*, vol. 14, no. 4, pp. 397–410, 2005.
[15] H. Oh, A. Bilgin, and M. Marcellin, "Visually lossless encoding for JPEG2000," *IEEE Transactions on Image Processing*, to appear.
[16] D. Chandler and S. Hemami, "Effects of natural images on the detectability of simple and compound wavelet subband quantization distortions," *Journal of the Optical Society of America A*, vol. 20, no. 7, pp. 1164–1180, 2003.
[17] H. Oh, A. Bilgin, and M. W. Marcellin, "Visually lossless JPEG2000 at fractional resolutions," in *IEEE International Conference on Image Processing*, 2011, pp. 309–312.
[18] D. Brainard, "The psychophysics toolbox," *Spatial vision*, vol. 10, no. 4, pp. 433–436, 1997.
[19] F. Auli-Llinas. (2012) BOI software. [Online]. Available: http://www.deic.uab.es/~francesc